Sandia National Laboratories

Albuquerque, New Mexico 87185

date: February 5, 1993

to: Distribution

from: D. W. Barnette, 1554

subject: Program **shocks**: Quickly estimating super- and hypersonic inviscid flow parameters

Introduction

Many times in the past, there has been a need to quickly estimate super- and hypersonic inviscid flow parameters for sphere, wedge, cone, and/or tangent sphere-cone shapes. This need has arisen for air as well as other gases. Such estimates are useful for determining outer boundary locations for computational meshes, shock impingement locations, stagnation heating rates, validation of more sophisticated computational or experimental results, and more. Undoubtedly, the NACA 1135 tables[1] are the most common source for such estimates, but these tables are not always handy, do not give all the information sometimes needed (shock standoff, heating rates, gases other than air), and are somewhat time consuming when performing table and chart look-ups, then cross-referencing to the numerical tables for additional calculations. Other sources of tabulated data exist for cones and spheres but suffer the same shortcomings.[2-5] Program **shocks** was developed to provide these capabilities and more.

Program **shocks** was initiated by my first researching various authors in super- and hypersonic flows.[6-16] Approximate governing equations for perfect-gas, high-speed flows over wedges, cones, and spheres were extracted from the texts, simplified if necessary, and programmed first on an HP-41CV hand calculator for convenience and initial testing. The comparisons with NACA 1135 tables and other results (to be presented) were, in most cases, so close for many regimes that I decided to program all of the equations into one code on the 1550 LAN. The exact equations were also programmed, *i.e.*, the Rankine-Hugoniot relations for a wedge and the Taylor-Maccoll relations for a cone. Results from these equations are output side-by-side with the approximate results. If desired, the user can then determine if the approximate relations provide close enough estimates for later use.

As mentioned above, the exact solutions are solved along side the approximate relations. Solving the exact relations requires more work, of course. As will be discussed, the Rankine-Hugoniot relations for wedges require a root finding technique to solve for the shock angle; the set of first-order ordinary differential Taylor-Maccoll equations for cones require numerical integration. On the other hand, the approximate algebraic relations, also

discussed below, provide direct computation of the shock angle. Hence, their implementation in a hand-held calculator can be easily accomplished.

Parameters for 16 different gases were installed in the code. The gases are air, ammonia, argon, butane, carbon dioxide, carbon monoxide, ethane, ethylene, helium, hydrogen, methane, nitrogen, octane, oxygen, sulfur dioxide, and water vapor.

The code was initially distributed among four staff members for check-out (F. G. Blottner, 1511; G. F. Homicz, 1511; A. R. Lopez, 1511; and J. L. Payne, 1554). Some coding errors were discovered and corrected, and helpful suggestions were made. It is now available for general use.

How to Run Program SHOCKS

Program **shocks** resides in the `/home/public/bin` directory on the 1500 LAN. Type **shocks** and the program will start (first-time users should type 'rehash' first, or perform a logout/login procedure). Input is simple and self explanatory. Obvious input errors are noted on the screen and the user is given repeated chances to correct the information. The source code resides in the `/home/public/etc` directory. English units are used, with no apologies. If there is a mighty uproar over units, I will be happy to add conversion factors.

Governing Equations

The following text discusses the approximate governing equations for a wedge, cone, and a sphere. The Rankine-Hugoniot relations for a wedge and the Taylor-Maccoll equations for a cone, the 'exact' relations, are also discussed. The equations for a sphere and a cone are used to estimate the flow parameters for a sphere-cone. No single set of equations was found for a sphere-cone geometry *per se*. The main assumptions for the approximate equations are inviscid, constant density flow. By the term 'constant density' is meant that the density of the flow between the body and shock (away from stagnation regions) is approximately constant. As will be seen, this turns out to be a surprisingly good assumption for super- and hypersonic flows over these types of geometries.

A common flow parameter found in the following equations is the density behind the shock, ρ_{sh}, ratioed to the freestream density, ρ_∞. The ratio is, by definition, called ε and is given by

$$\varepsilon = \frac{\rho_{sh}}{\rho_\infty} = \frac{\gamma - 1}{\gamma + 1}\left(1 + \frac{2}{(\gamma - 1)\, M_\infty^2 \sin^2\beta}\right) \qquad (1)$$

where β is the shock angle and is the unknown. The following equations will give estimated or exact values for the shock angle, after which ε can be calculated knowing the specific heat ratio, γ, and the freestream mach number, M_∞. This then allows other appropriate flow parameters to be determined, such as the pressure coefficient.

Wedge Flow

a) Approximate Relations for the Wedge

The objective of the wedge flow calculations is as follows. Let the subscript '*w*' imply '*wedge.*' Given the wedge angle, θ_w, the freestream Mach number, M_∞, and the wedge length, L_w, calculate the shock angle, β_w, the surface pressure ratioed to the freestream pressure, P_w/P_∞, the surface pressure coefficient, $C_{p,w}$, and the shock height at the back of the wedge, H_w.

Consider the following schematic for wedge flow (also to be used for cone flow, later):

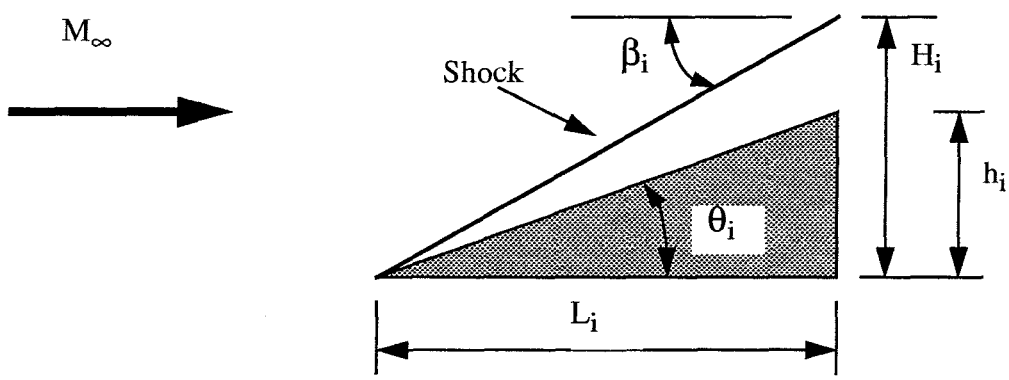

Figure 1. Parameters used for wedge (i='w') and cone (i='c') flow relations.

Knowing the wedge angle, θ_w, one can calculate the approximate shock angle by the equation from Hayes and Probstein,[6] (pp. 140-2)

$$\beta_w = \frac{(\gamma+1)\,\theta_w}{4} + \sqrt{\left(\frac{(\gamma+1)\,\theta_w}{4}\right)^2 + \frac{1}{M_\infty^2}} \quad . \tag{2}$$

This allows the density ratio ε, given in Eq. 1, to be determined. Then the pressure coefficient at the surface, which for wedge flow is equivalent to that behind the shock, is given by

$$C_{p,w} = \frac{2\theta_w^2}{(1-\varepsilon)} \quad . \tag{3}$$

The base height, h_w, and the shock height, H_w, for the wedge are given respectively by the simple relations

$$h_w = L_w \tan\theta_w \tag{4}$$

and

$$H_w = L_w \tan\beta_w \quad . \tag{5}$$

b) Exact Relations for the Wedge

The Rankine-Hugoniot, or 'shock-jump', relations are used to calculate 'exact' parameters on a wedge. From the NACA 1135 tables,[1] the equation for the shock angle, β_w, is given implicitly by

$$\sin^6\beta_w - \left(\frac{M_\infty^2+2}{M_\infty^2} + \gamma\sin^2\theta\right)\sin^4\beta_w$$

$$+\left(\frac{2M_\infty^2+1}{M_\infty^4} + \left(\frac{(\gamma+1)^2}{4} + \frac{\gamma-1}{M_\infty^2}\right)\sin^2\theta_w\right)\sin^2\beta_w - \frac{\cos^2\theta_w}{M_\infty^4} = 0 \quad . \tag{6}$$

A secant root finding method is used in program **shocks** to solve for β_w, with the initial guess to the root coming from the approximate relations. There are three positive (and three negative) roots, so the initial guess should be close to the expected outcome. Convergence appears to be very fast, usually within 10 search cycles. Once the shock angle is known, equations listed in NACA 1135 and programmed in **shocks** can be used to determine other relevant parameters.

Cone Flow

a) Approximate Relations for the Cone

The objective of the cone flow calculations is as follows. Let the subscript '*c*' imply '*cone.*' Given the cone angle, θ_c, the freestream Mach number, M_∞, and the cone length, L_c, calculate the shock angle, β_c, the surface pressure ratioed to the freestream pressure, P_c/P_∞, the surface pressure coefficient, $C_{p,c}$,and the shock height at the back of the cone, H_c.The previous schematic for wedge flow can be used for cone flow if one considers that only half of the cone

is drawn and that a 'slice' of the flow field is shown. The approximate expression for the shock angle for a cone is given by Hayes and Probstein[6] (p. 150) as

$$\beta_c - \theta_c = \frac{1}{2}\left(\frac{\gamma-1}{\gamma+1}\left(1+\frac{2}{M_\infty^2\beta_c^2(\gamma-1)}\right)\right)(1+\frac{\varepsilon}{12})\,\beta_c \quad .$$

As it stands, the above equation is an implicit function of the shock wave angle, β_c. Obviously, a root finding method could be used to extract β_c, but again this is beyond the scope of quickly estimating flow parameters from 'approximate' relations. I derived a simpler algebraic relation as follows. Substituting for the density ratio, ε (which itself is a function of β_c), assuming 'small' shock angles, and expanding and collecting terms, one can write the above equation as

$$\underset{O(10^{-4})}{\left(1-\frac{13\gamma^2-2\gamma-11}{24(\gamma+1)^2}\right)\beta_c^4} \underset{O(10^{-4})}{-\theta_c\beta_c^3} \underset{O(10^{-5})}{-\left(\frac{14\gamma+10}{12(\gamma+1)^2M_\infty^2}\right)\beta_c^2} \underset{O(10^{-6})}{-\frac{1}{6(\gamma+1)^2M_\infty^4}} = 0 \quad . \tag{8}$$

An order-of-magnitude analysis indicates the last term is a higher-order term and can be ignored for 'large' Mach numbers and 'moderate' cone and shock angles. The third term could also be considered of higher-order. However, to ignore this <u>and</u> the last term is to remove all dependence on the Mach number, which is undesirable. Neglecting only the last term conveniently drops the 4-th order polynomial to a quadratic, the solution of which is given by

$$\beta_c = \frac{\theta_c + \sqrt{\theta_c^2 + \dfrac{154\gamma^3+810\gamma^2+990\gamma+350}{72(\gamma+1)^4M_\infty^2}}}{\dfrac{11\gamma^2+50\gamma+35}{12(\gamma+1)^2}} \quad . \tag{9}$$

The surface pressure ratio is given by

$$\frac{P_c}{P_\infty} = 1 + C_{p,c}\frac{\gamma}{2}M_\infty^2 \tag{10}$$

where the surface pressure coefficient is given by

$$C_{p,c} = \frac{2\sin^2\theta_c}{(1-\frac{\varepsilon}{4})\cos^2(\beta_c-\theta_c)} \quad . \tag{11}$$

The base height, h_c, and the shock height, H_c, for the cone are given respectively by the simple relations

$$h_c = L_c \tan\theta_c \tag{12}$$

and

$$H_c = L_c \tan\beta_c \quad . \tag{13}$$

b) Exact Relations

The exact relations consist of a set of first order, ordinary differential equations that describe the flow between the body and shock about a sharp cone. These equations were first solved by numerical integration by Taylor and Maccoll[16] and require an iterative approach to finding the shock angle for a given freestream Mach number. The equations and somewhat lengthy solution procedure are discussed in Shapiro[8] and will not be repeated here.

Sphere and Tangent Sphere-Cone Flow

The objective of the tangent sphere-cone flow calculations is as follows. As indicated in Fig. 2, let the subscript '*sc*' imply '*sphere-cone*.' Given the nose radius, R_n, the cone angle, θ_{sc}, the freestream Mach number, M_∞, and the sphere-cone length, L_{sc}, calculate the shock standoff at the nose, Δ, the stagnation density ratio behind the shock, ρ_{t2}/ρ_∞, the stagnation pressure ratio behind the shock, p_{t2}/p_∞, the shock angle on the cone, β_{sc}, the surface pressure ratioed to the freestream pressure, p_{sc}/p_∞, the surface pressure coefficient, $C_{p,sc}$, and the shock height at the back of the cone, H_{sc}. The stagnation point heat transfer rate, q_{sc}, can also be calculated, provided the following are known: freestream temperature, T_∞, the wall temperature, T_w, and the freestream density, ρ_∞.

Only the flow near the stagnation region will be discussed in detail since the equations for the conical portion are identical to those for cone flow, above, and will not be repeated here. The conical portion of the flow field is calculated assuming a virtual cone whose length,

$L_{virtual}$, is what it would be with an extended sharp nose, not the spherical nosecap. This approximation implies that the equations for cone flow will more accurately model the flow at the end of a sphere-cone the longer the sphere-cone and the smaller its bluntness ratio, R_n/h_{sc}, where h_{sc} is the base radius.

Program **shocks** also provides the option of running only sphere calculations. If this option were always run with the cone calculations, results for the sphere would not be output if the code failed to calculate an attached shock for the virtual cone.

Consider the following schematic for the stagnation region of tangent sphere-cone flow:

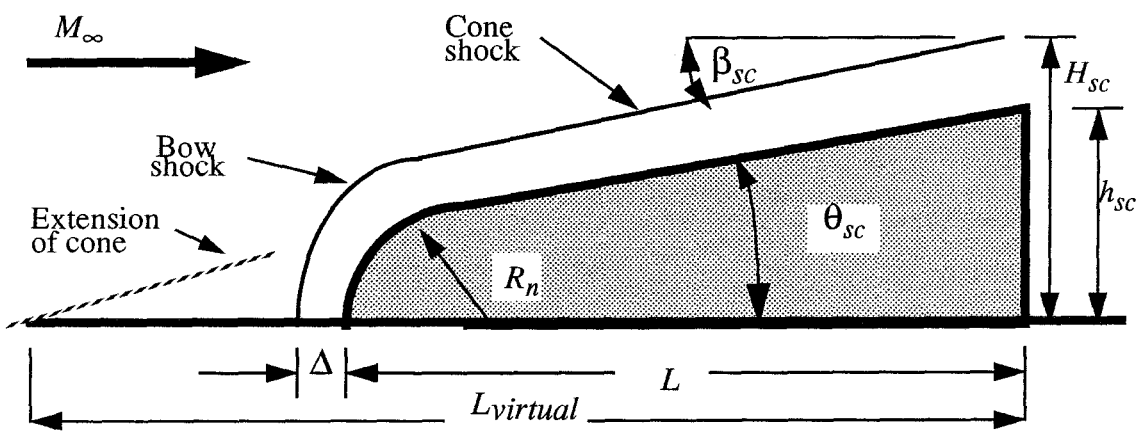

Figure 2. Parameters used for sphere and tangent sphere-cone flow relations.

From Lomax and Inouye,[12] the equation for the shock standoff distance is given by

$$\Delta = 0.85\left(\frac{\rho_\infty}{\rho_{t2}}\right)R_n \tag{14}$$

where the stagnation density ratio is given by

$$\frac{\rho_{t2}}{\rho_\infty} = \left[\frac{(1+\frac{1}{2}(\gamma-1)M_\infty^2)}{\frac{p_{t2}}{p_\infty}}\right]^{-1} \tag{15}$$

and the stagnation pressure ratio is given by

$$\frac{p_{t2}}{p_\infty} = \left(\frac{1}{2}(\gamma+1)M_\infty^2\right)^{\frac{\gamma}{\gamma-1}} \left(\frac{\gamma+1}{2\gamma M_\infty^2-\gamma+1}\right)^{\frac{1}{\gamma-1}} \quad . \tag{16}$$

The shock angle, surface pressure ratio, and surface pressure coefficient equations for the conical portion of the vehicle are the same as those presented in the section **Cone Flow**. However, for the sphere-cone, these relations are based on the virtual length of the conical portion of the sphere-cone, given by

$$L_{virtual} = L + x_t - \frac{z_t}{\tan\theta_{sc}} \quad . \tag{17}$$

The variables x_t and z_t represent the coordinates of the sphere-cone tangency point, where

$$x_t = R_n(1-\sin\theta_s) \tag{18}$$

and

$$z_t = R_n\cos\theta_s \quad . \tag{19}$$

The base height, h_{sc}, and the shock height, H_{sc}, for the cone are given respectively by the simple relations

$$h_{sc} = L_{virtual}\tan\theta_{sc} \tag{20}$$

and

$$H_{sc} = L_{virtual}\tan\beta_{sc} \quad . \tag{21}$$

Stagnation point heat transfer results are obtained using the Fay and Riddell relation, as discussed in White[9] (p. 597), *i.e.*,

$$\dot{q}_w = 0.763Pr^{-0.6}(\rho_{t2}\mu_{t2}K)^{1/2}\left(\frac{\rho_w}{\rho_{t2}}\frac{\mu_w}{\mu_{t2}}\right)^{0.1} C_p(T_{t2}-T_w) \quad \frac{Btu}{ft^2\text{-}sec} \quad . \tag{22}$$

For generality, the Prandtl number for a perfect gas is given by White[9] (p. 32) as

$$Pr = \frac{4\gamma}{7.08\gamma - 1.80} \quad . \tag{23}$$

The well-known relation for stagnation temperature is given by

$$\frac{T_{t2}}{T_\infty} = 1 + \frac{(\gamma - 1)}{2} M_\infty^2 \quad . \tag{24}$$

The coefficient of dynamic viscosity is calculated using Sutherland's formula

$$\mu = C_1 \left(\frac{T^{3/2}}{T + C_2} \right) \qquad \frac{lbf\text{-}sec}{ft^2} \tag{25}$$

and C_1 and C_2 are constants for a particular gas. These constants are listed in Table 1 for the gases implemented in the program. Finally, the velocity gradient 'K' is determined by the equation

$$K = \frac{V_\infty}{2R_n} \sqrt{C \frac{\rho_\infty}{\rho_{t2}}} \tag{26}$$

where C=8.0 for all gases except air. For air, White[9] (p. 599) states that C=7.4 gives better results. Hence, **shocks** is programmed to use the appropriate value.

A constant value for the specific heat, C_p, for each gas has been implemented. Values for C_p are also listed in Table 1.

Comparisons of Results with Other Data

The simplest validation exercise is to compare calculated results from the **shocks** code with NACA 1135 tables. This will show how well the equations presented above approximate the flow.

Presented in Table 2 are results for wedges. Combinations of both small and large wedge angles and Mach numbers are represented. The calculated error shown below the results for each case gives an indication of the accuracy of **shocks**. Results are acceptable for estimation purposes over a wide range of input parameters.

Presented in Table 3 are results for sharp cones. Again, combinations of both small and large wedge angles and Mach numbers are represented. And again, results are acceptable for estimation purposes over a wide range of input parameters.

Stagnation properties from program **shocks** were compared with results from Blottner's[14] blunt body code NS3D for air. Results are presented in Table 4. Blottner's code gives results at the wall, while **shocks** can give only the stagnation flow conditions. Hence, comparisons can show large differences for stagnation density, for example, which is a function of wall temperature. For stagnation pressure, however, comparisons show excellent agreement.

Properties for sphere-cones listed in Table 4 are estimated by using the cone equations for a virtual length cone, as has been discussed. Estimates for shock standoff at the base become more accurate for longer sphere-cones since the flow gradually returns to conical flow downstream of the stagnation point.

Table 5 lists results for a sphere-cone obtained using the different gases implemented in program **shocks**. No experimental data are provided, since it is doubtful if data exists for all the gases for the same geometry and freestream conditions. This comparison is made simply to show how the different gases affect the properties calculated in **shocks**. Geometry particulars and freestream quantities are listed in the table's heading. Nomenclature is that used in Fig. 2.

The shock standoff distance, plotted as a function of the axial distance from the nose, of the two sphere-cone cases listed in Table 4 have been compared to that of the virtual cone calculations from program **shocks**. Recall that the two sphere-cone cases from Table 4 were computed by Walker[19] using the parabolized Navier-Stokes code SPRINT. The shock is numerically fitted in SPRINT, so the shock location is easily found from the solution. Program **shocks** provided Taylor-Maccoll solutions to determine the shock standoff for a virtual length cone. Recall that a virtual length cone is the shape of the sphere-cone from the SPRINT calculations if it had an extended, sharp nose. Comparison of these two numbers reveals the distance along the sphere-cone that the shock approaches that of a virtual length cone. This is dependent on Mach number, nose bluntness, and cone half-angle. Fig. 3 shows this comparison for both Mach numbers, 3 and 15. Shock standoff error, in %, is defined as

$$shock-standoff-error = 100\left(1-\frac{H_c-h_{sc}}{H_{sc}-h_{sc}}\right) \quad . \tag{27}$$

Here, H_c is the shock height above the centerline at the desired distance along the virtual length cone, H_{sc} is the shock height at the equivalent location along the sphere-cone as taken from the SPRINT code, and h_{sc} is the radius of the of the sphere-cone at that location. Results for Mach 3 indicate the sphere-cone shock approaches the cone shock to within 5% in 25 nose radii. However, for Mach 15, it requires approximately 250 nose radii before the shock approaches that of a cone within 5% error.

Summary

A computer code, **shocks**, has been programmed to estimate super- and hypersonic inviscid flow parameters for spheres, wedges, cones, and tangent sphere-cones. Comparisons have been made with NACA 1135 tables, computational fluid dynamics codes, and data in the literature. Within the limitations of the approximate and 'exact' equations, program **shocks** provides a fast method for estimating flow parameters with engineering accuracy. The code will be particularly useful for estimating outer grid boundaries for high-speed flow solutions using CFD codes, shock impingement locations, heating rates for wind tunnel and flight conditions, and more for a wide variety of gases.

The program is executed by typing **shocks** on the 1500 LAN. Input is simple and self-explanatory. Run time is typically a few seconds.

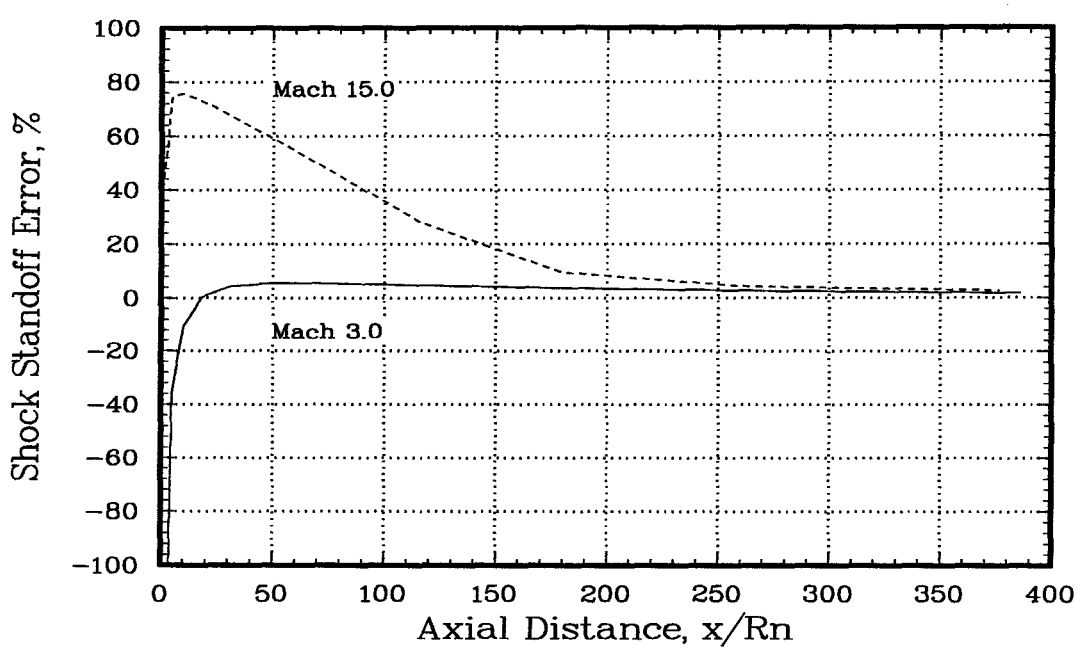

Figure 3. Comparison of shock standoff error for a cone and tangent sphere-cone for Mach numbers 3 and 15.

References

1. "Equations, Tables, and Charts for Compressible Flow," NACA Report 1135, Ames Research Staff, Ames Aeronautical Laboratory, Moffett Field, California.

2. D. J. Jones, "Numerical Solutions of the Flow Field for Conical Bodies in a Supersonic Stream," Aeronautical Report LR-507, National Research Council of Canada, Ottawa, July 1968.

3. J. L. Sims, "Tables for Supersonic Flow Around Right Circular Cones at Zero Angle of Attack," NASA SP-3004, 1964.

4. J. L. Sims, "Tables for Supersonic Flow Around Right Circular Cones at Small Angle of Attack," NASA SP-3007, 1964.

5. A. N. Lyubimov and V. V. Rusaniv, "Gas Flows Past Blunt Bodies, Part I: Calculation Method and Flow Analysis," NASA TT F-714, and "Part II: Tables of the Gasdynamic Functions," NASA TT F-715, February 1973.

6. W. D. Hayes and R. F. Probstein, Hypersonic Flow Theory, Academic Press, 1959.

7. R. N. Cox and L. F. Crabtree, Elements of Hypersonic Aerodynamics, Academic Press, 1965.

8. A. H. Shapiro, The Dynamics and Thermodynamics of Compressible Fluid Flow, The Ronald Press Company, New York, 1954.

9. F. M. White, Viscous Fluid Flow, McGraw-Hill Book Company, 1974.

10. W. H. Giedt, Principles of Engineering Heat Transfer, D. Van Nostrand Company, Inc., 1957.

11. A. J. Chapman, Heat Transfer, 3rd edition, Macmillan Publishing Company, 1974.

12. H. Lomax and M. Inouye, "Numerical Analysis of Flow Properties About Blunt Bodies Moving at Supersonic Speeds in an Equilibrium Gas," NASA TR R-204, July 1964.

13. E. R. G. Eckert and R. M. Drake, Heat and Mass Transfer, McGraw-Hill Book Company, Inc., 1959.

14. F. G. Blottner, "Accurate Navier-Stokes Results for the Hypersonic Flow over a Spherical Nosetip," *Journal of Spacecraft and Rockets*, Vol. 27, No. 2, March-April, 1990, pp. 113-122.

15. N. F. Krasnov, Aerodynamics of Bodies of Revolution, American Elsevier Publishing Company, Inc., New York, 1970.

16. G. I. Taylor and J. W. Maccoll, "The Air Pressure on a Cone Moving at High Speed," *Proc. Roy. Soc.* (A), Vol. 139 (1933), p. 278.

17. R. C. Reid, J. M. Prausnitz, and T. K. Sherwood, The Properties of Gases and Liquids, McGraw-Hill Book Company, 1977.

18. Handbook of Chemistry and Physics, The Chemical Rubber Company, 49th edition, 1968.

19. M. A. Walker (Dept. 1511), private transmittal, Sandia/New Mexico, December 18, 1992.

Table 1. Parameters for gases used in program *shocks*.

#	Gas	Specific Heat Ratio, γ	C_p (Btu/lbm-°R)	R (ft²/sec²-°R)	C_1 for Sutherland law, Eq. 25	C_2 for Sutherland law, Eq. 25	References
1	air	1.40	0.240	1716.26	2.270e-08	198.7	10, 11
2	ammonia	1.29	0.520	2920.54	2.40e-08	849.0	10, 11
3	argon	1.68	0.124	1247.11	3.029e-08	265.7	10, 18
4	butane	1.09	0.406	856.84	1.529e-08	673.8	10, 17
5	carbon dioxide	1.29	0.201	1130.86	2.420e-08	420.0	10, 11
6	carbon monoxide	1.40	0.248	1777.12	2.180e-08	196.0	10, 11
7	ethane	1.19	0.418	1656.05	1.568e-08	473.8	10, 18
8	ethylene	1.25	0.360	1775.19	1.627e-08	409.6	10, 18
9	helium	1.67	1.250	12439.83	2.360e-08	176.0	10, 11
10	hydrogen	1.41	3.416	24682.27	1.010e-08	127.0	10, 11
11	methane	1.30	0.532	3104.08	1.530e-08	279.0	10, 11
12	nitrogen	1.40	0.248	1775.83	2.160e-08	184.0	10, 11
13	octane	1.04	0.407	435.99	1.039e-08	613.6	10, 18
14	oxygen	1.39	0.219	1554.94	2.570e-08	198.0	10, 11
15	sulfur dioxide	1.25	0.154	766.66	2.682e-08	717.0	10, 18
16	water vapor (steam)	1.33	0.445	2756.32	2.715e-08	1146.2	10, 13

Table 2. Comparisons for wedges in air.

Wedge angle, θ_w (degs) ↓ / M_∞ →		2.0		5.0		20.0	
		Shock angle, β_w (degs)	Surface pressure coeff., $C_{p,w}$	Shock angle, β_w (degs)	Surface pressure coeff., $C_{p,w}$	Shock angle, β_w (degs)	Surface pressure coeff., $C_{p,w}$
5.0	**shocks** code	31.81	0.1829	14.84	0.0468	7.14	0.0218
	Rankine-Hugoniot	34.30	0.1126	15.07	0.0460	7.15	0.0217
	error,%	7.28	-62.38	1.50	-1.63	0.15	-0.35
10.0	**shocks** code	35.27	0.2922	18.93	0.1179	12.64	0.0771
	Rankine-Hugoniot	39.31	0.2523	19.37	0.1168	12.70	0.0765
	error,%	10.28	-15.80	2.27	-0.95	0.46	-0.85
20.0	**shocks** code	43.06	0.6306	28.59	0.3543	24.33	0.2968
	Rankine-Hugoniot	53.42	0.6582	29.80	0.3450	24.69	0.2867
	error,%	19.39	4.18	4.05	-2.70	1.44	-3.51
30.0	**shocks** code	51.83	1.1048	39.33	0.7307	36.22	0.6627
	Rankine-Hugoniot	detached	n/a	42.34	0.6895	37.54	0.6147
	error,%	n/a	n/a	7.10	-5.97	3.50	-7.82

Table 3. Comparisons for cones in air.

Cone half-angle, θ_c (degs) ↓ / M_∞ →		2.0		5.0		20.0	
		Shock angle, β_c (degs)	Surface pressure coeff., $C_{p,c}$	Shock angle, β_c (degs)	Surface pressure coeff., $C_{p,c}$	Shock angle, β_c (degs)	Surface pressure coeff., $C_{p,c}$
5.0	**shocks** code	22.51	0.0277	11.03	0.0210	6.09	0.0167
	Taylor-Maccoll	30.10	0.0337	12.30	0.0232	6.20	0.0171
	error,%	25.21	17.69	10.32	9.57	1.75	2.82
10.0	**shocks** code	25.80	0.0953	15.01	0.0729	11.26	0.0639
	Taylor-Maccoll	31.20	0.1046	15.60	0.0751	11.40	0.0649
	error,%	17.30	8.92	3.76	3.05	1.20	1.57
20.0	**shocks** code	33.35	0.3144	24.36	0.2588	22.02	0.2454
	Taylor-Maccoll	37.80	0.3263	25.00	0.2617	22.20	0.2468
	error,%	11.76	3.64	2.53	1.11	0.81	0.58
30.0	**shocks** code	41.92	0.6206	34.54	0.5396	32.88	0.5240
	Taylor-Maccoll	48.20	0.6475	35.70	0.5446	33.40	0.5269
	error,%	13.02	4.16	3.23	0.90	1.54	0.54

Table 4. Comparison of sphere and tangent sphere-cone results for air.

Geometry and conditions (↓) / Quantity (→)		Sphere				Virt. length cone: Approximate (Taylor-Maccoll)		
		Stagnation pressure ratio, p_{t2}/p_∞	Stagnation density ratio, ρ_{t2}/ρ_∞	Shock stand-off at nose, Δ (in)	Heat flux at nose, q (Btu/ft^2-sec)	Shock angle at back of cone, β_{sc} (deg)	Shock stand-off at back of cone, H_{sc}-h_{sc} (in)	Surface pressure coefficient, $C_{p,sc}$
Sphere M_∞=5.0 Re_∞=3.775e05 per inch T_w=178.0 °R T_∞=136.1 °R R_n=2.5 in.	**shocks** code	32.65	5.44	-0.3905	9.474	---	---	---
	Blottner, Ref. 14	32.65	24.97	-0.3949	9.473	---	---	---
	error,%	0.00	78.21	1.11	-0.01	---	---	---
Sphere-cone M_∞=15.0 Re_∞=2.724e05 per inch T_w=3000 °R T_∞=400.4 °R R_n=0.4 in. L_{sc}=3.86 in. θ_{sc}=5.25° h_{sc}=0.7196 in.	**shocks** code	290.16	6.30	-0.0539	2177.59	6.74 (6.85)	0.2068 (0.2212)	0.0188 (0.0193)
	Walker, Ref. 19	289.56	38.65	-0.0530	2178.61	11.05	0.9132	0.0213
	error,%	-0.21	83.70	-1.70	0.05	39.00 (38.01)	77.35 (75.78)	11.74 (9.39)
Same as above, but L_{sc}=37.11 in., h_{sc}=3.7749 in.	**shocks** code	Sphere properties same as above				6.74 (6.85)	1.0846 (1.1601)	0.0188 (0.0193)
	Walker, Ref. 19					5.75	1.9034	0.0164
	error,%					-17.22 (-19.13)	43.02 (39.05)	-14.63 (-17.68)
Same as above, but L_{sc}=130.51 in., h_{sc}=12.357 in.	**shocks** code	Sphere properties same as above				6.74 (6.85)	3.5507 (3.7979)	0.0188 (0.0193)
	Walker, Ref. 19					6.84	3.9226	0.0192
	error,%					1.46 (-0.15)	9.48 (3.18)	2.08 (-0.52)
Sphere-cone M_∞=3.0 Re_∞=5.448e05 per inch T_w=1000 °R T_∞=400.4 °R R_n=0.4 in. L_{sc}=47.69 in. θ_{sc}=5.25° h_{sc}=4.7472 in.	**shocks** code	12.061	4.307	-0.0789	2.950	16.24 (19.75)	10.30 (13.80)	0.0262 (0.0306)
	Walker, Ref. 19	12.075	4.835	-0.0885	3.213	20.11	14.47	0.0308
	error,%	0.12	10.92	10.85	8.19	19.24 (1.79)	28.82 (4.63)	14.94 (0.65)

Table 5. Comparisons for gases represented in program *shocks*. Values are for a sphere-cone, M_∞=8, R_n=0.5 *in.*, θ_{sc}=15°, L_{sc}=60 *in.*, T_∞=400°R, T_w=2500°R, sea level, h_{sc}=16.46 *in.*

Quantity → / Gas ↓	Sphere				Cone (Taylor-Maccoll)		
	Stagnation pressure ratio, p_{t2}/p_∞	Stagnation density ratio, ρ_{t2}/ρ_∞	Shock stand-off at nose, Δ (in)	Heat flux at nose, q (btu/ft^2-sec)	Shock angle, β_{sc} (deg)	Shock stand-off at back of cone, H_{sc}-h_{sc} (in))	Surface pressure coefficient, $C_{p,sc}$
Air	82.86	6.00	-0.0708	1135.43	18.00	3.50	0.1471
Ammonia	77.95	7.58	-0.0560	1360.99	17.60	3.03	0.1453
Argon	95.01	4.17	-0.1018	1580.54	18.80	4.45	0.1502
Butane	68.76	17.72	-0.0240	-296.47	17.00	2.32	0.1430
Carbon dioxide	77.95	7.58	-0.0560	438.02	17.60	3.02	0.1453
Carbon monoxide	82.86	6.00	-0.0708	1160.18	18.00	3.50	0.1471
Ethane	73.40	10.36	-0.0410	151.67	17.30	2.67	0.1442
Ethylene	76.14	8.46	-0.0502	477.30	17.50	2.91	0.1450
Helium	94.59	4.21	-0.1008	24633.19	18.80	4.45	0.1503
Hydrogen	83.30	5.90	-0.0720	22608.21	18.00	3.50	0.1470
Methane	78.40	7.39	-0.0575	1312.39	17.70	3.14	0.1460
Nitrogen	82.86	6.00	-0.0708	1156.12	18.00	3.50	0.1471
Octane	66.40	29.12	-0.0146	-308.86	16.80	2.09	0.1421
Oxygen	82.42	6.11	-0.0695	1044.45	18.00	3.50	0.1472
Sulfur dioxide	76.14	8.46	-0.0502	204.25	17.50	2.91	0.1450
Water vapor	79.74	6.89	-0.0616	1611.38	17.80	3.26	0.1464

Distribution:

1500	D. J. McCloskey
1501	C. W. Peterson
1502	P. J. Hommert
1503	L. W. Davison
1511	J. S. Rottler
	Attn: Staff
1511	F. G. Blottner
1511	G. F. Homicz
1511	M. A. Walker
1511	C. C. Wong
1512	A. C. Ratzel
	Attn: Staff
1513	R. D. Skocypec
	Attn: Staff
1551	W. P. Wolfe
	Attn: Staff
1552	C. E. Hailey
	Attn: Staff
1553	W. L. Hermina
	Attn: Staff
1553	D. L. Potter
1554	W. H. Rutledge
	Attn: Staff
1554	E. L. Clark
1554	J. L. Payne
1561	H. S. Morgan
	Attn: Staff
1562	R. K. Thomas
	Attn: Staff
9814	R. W. Greene
9816	R. E. Sheldahl

Copy to:

1554	Day File